Contrast-Enhanced Harmonic Ultrasonography for the Assessment of Prostate Cancer Aggressiveness: a Preliminary Study

Yunkai Zhu, MD[1]
Yaqing Chen, MD[1]
Jun Jiang, MD[1]
Ren Wang, MD[2]
Yongchang Zhou, MD[2]
Huizhen Zhang, MD[3]

Index terms:
Prostate neoplasms
Transrectal ultrasound
Contrast agents
Gleason score

DOI:10.3348/kjr.2010.11.1.75

Korean J Radiol 2010;11:75-83
Received June 7, 2009; accepted after revision August 10, 2009.

[1]Department of Ultrasound in Medicine, Xinhua Hospital Affiliated to Shanghai Jiaotong University School of Medicine, 1665 Kongjiang Road, Shanghai, 200092, P.R China; [2]Department of Ultrasound in Medicine, Sixth People's Hospital Affiliated to Shanghai Jiaotong University, 600 Yishan Road, Shanghai, 200233, P.R China; [3]Department of Pathology, Sixth People's Hospital Affiliated to Shanghai Jiaotong University, 600 Yishan Road, Shanghai, 200233, P.R China

This work was supported by a grant from Science and Technology Commission of Shanghai Municipality (034119947).

Address reprint requests to:
Yaqing Chen, MD, Department of Ultrasound in Medicine, Xinhua Hospital Affiliated to Shanghai Jiaotong University School of Medicine, 1665 Kongjiang Road, Shanghai, 200092, P.R China.
Tel. (+86 21) 65790000
Fax. (+86 21) 65790000-5350
e-mail: joychen1266@126.com;
tttmax2004@hotmail.com

Objective: To determine whether contrast-enhanced harmonic ultrasonography can be used to predict the aggressiveness of prostate cancer.

Materials and Methods: Contrast-enhanced harmonic ultrasonography was performed in 103 patients suspected of prostate cancer before biopsy. Time intensity curves were reconstructed for systematic biopsy sites and sonographic abnormalities. The characteristics of the curves were described using hemodynamic indices including arrival time (AT), time-to-peak (TTP), and peak intensity (PI). The differences of hemodynamic indices between high-grade and low-grade cancer were analyzed and the correlations between the hemodynamic indices and biopsy Gleason score were studied.

Results: Prostate cancer was detected in 41 of 103 patients and there were significant differences in the hemodynamic indices between the biopsy sites of the non-malignant patients and prostate cancer lesions ($p < 0.05$). The prostate biopsies revealed 154 prostate cancer lesions, including 31 low-grade lesions and 123 high-grade lesions. The hemodynamic indices AT and TTP of high-grade tumors were significantly shorter than those of low-grade tumors (p = 0.001, 0.002). In addition, high-grade peripheral zone (PZ) tumors had higher PI than low-grade PZ tumors ($p = 0.009$). The PZ prostate cancer Gleason score correlated with PI, AT and TTP, with Spearman correlation coefficients of 0.223, −0.335, and −0.351, respectively (p = 0.013, < 0.001 and < 0.001).

Conclusion: Contrast-enhanced ultrasound measurements of hemodynamic indices correlate with the prostate cancer Gleason score.

In patients with prostate cancer, the accurate assessment of tumor aggressiveness is important in the treatment decision-making and prognosis prediction. A prostate biopsy Gleason score is widely used in assessing prostate cancer aggressiveness. Recent studies have found that prostate cancer lesions with higher Gleason scores had a higher degree of vascularity (1, 2). Thus, an imaging protocol which can assess microvasculature will be useful in predicting prostate cancer Gleason score noninvasively.

Microbubble contrast agents provide a practical solution to the problem of imaging microvasculature in the prostate (3–6). With contrast-enhanced targeted biopsy, the prostate cancer detection rate can be improved with fewer cores (7–9). Also, another study found that contrast-enhanced ultrasonography was more sensitive in detecting higher grade tumors (10) and the author suggested that contrast-enhanced ultrasound might be helpful in grading the prostate cancer. In this paper, contrast-enhanced harmonic ultrasonography was employed to facilitate an accurate analysis of the time intensity curve and hemodynamic indices of the prostate gland. The purpose of this

study is to determine whether contrast-enhanced ultrasonography and the hemodynamic parameter is useful in predicting prostate cancer Gleason score.

MATERIALS AND METHODS

Study Population

The study was performed according to the ethical standards of the Institutional Review Board, and informed consent was obtained from each patient. A total of 103 consecutive male subjects underwent transrectal ultrasound-guided prostate biopsies for the first time due to either abnormal digital rectal examination findings or elevated serum prostate specific antigen (PSA) levels ($\geq$ 4 ng/ml). A contrast-enhanced ultrasonography was performed for each patient before the biopsy.

Imaging Protocol

A radiologist with 10 years experience in performing transrectal ultrasound and prostate biopsies performed all the ultrasonography examinations with the Sequoia 512 (Siemens Medical Solutions, Mountain View, CA) ultrasonography system equipped with EV8C4-S end-fire probe. All patients were examined in the left lateral decubitus position. Gray-scale imaging was performed with a probe frequency of 7.0 MHz, a dynamic range of 80 dB. For color Doppler ultrasonography, the probe frequency was 6.0 MHz, the color Doppler gain was adjusted to maximize the signal but eliminate color noise from the tissue of the prostate, and the color Doppler window was set to include the entire gland. After the baseline ultrasonography, a contrast-enhanced ultrasonography was performed using cadence contrast pulse sequencing (CPS) mode, with a probe frequency of 8.0 MHz, a dynamic range of 81 dB, a mechanical index of 0.11, and a CPS gain setting with automatic optimizing. For contrast-enhanced ultrasonography, two planes were scanned for each patient: one being the transverse plane of maximal width; the other was the transverse plane of the sonographic abnormality, or the most hypervascular plane on color Doppler imaging for patients with no suspicion of prostate cancer on baseline ultrasonography. For further spatial correlation within the biopsy site, the contrast imaging plane was saved using internal and external anatomic landmarks for references (i.e., veromontanum, external sphincter, surgical and anatomic capsule, urethra, neurovascular bundle, hypertrophic gland nodules, seminal vesicle, and hypoechoic lesions). The entire examination was saved in DICOM (digital imaging and communications in medicine) format and transmitted to a workstation for further analysis.

Contrast Infusion

Contrast-enhanced imaging was performed during the injection of a sulphur hexafluoride microbubble (SonoVue, Bracco, Italy) at a concentration of 8 ul/ml. A volume of 2.4 ml contrast agent was administered for each contrast plane. In addition a total volume of 4.8 ml contrast agent was administered to each patient for two contrast planes. The contrast agent was administered as a bolus via an

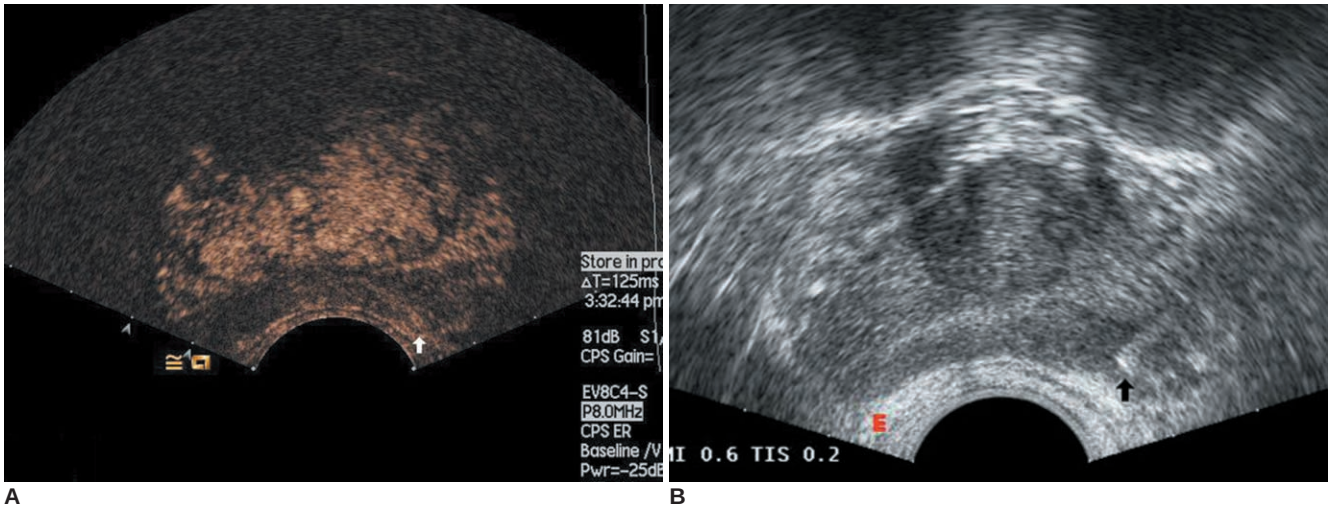

A B

Fig. 1. Figures showing biopsy procedure.
A. Postcontrast image of prostate gland of 68-year-old man with elevated prostate specific antigen level of 6.85 ng/ml. Substantial enhancement and earlier arrival of contrast-enhanced blood were observed in lateral part of left peripheral zone (arrow).
B. During biopsy, biplane probe was rotated to sagittal plane of area showing abnormal findings using anatomic landmarks as reference, after biopsy gun was fired, probe was switched to convex transducer. Biopsy site (black arrow, comet tail sign) was determined precisely at area showing abnormal findings. Biopsy revealed prostate lesion with Gleason score of 4 + 3.

antecubital vein of the right arm. Immediately after contrast injection, 5 ml of 0.9% sodium chloride was injected to clear the intravenous cannula.

Biopsy Protocol and Histopathologic Analysis

Prior to the biopsy, all patients underwent an evaluation for blood coagulation, urine analysis, and electrocardiogram. Anticoagulant therapy was stopped seven days before the procedure. In addition, prophylactic antibiotic coverage was not provided routinely except for patients with high risk of urinary tract infection, in which case, they would be provided with fluoroquinolone for three days beginning from the day before the biopsy. After the completion of the ultrasound examination, the ultrasound-guided transperineal prostate biopsies were performed using a Technos MPX (ESAOTE, Italy) scanner with a TRT23 biplane probe by two radiologists. Both the octant systematic biopsies and targeted biopsies were taken with a spring-loaded biopsy gun (BARD MAGNUM, Covington, GA) and an 18-gauge Tru-cut biopsy needle. With the patient in the lithotomy position the perineal area was disinfected and bilateral local anesthesia was administered with 10 ml of 2% lidocaine solution. The 8-core based biopsy strategy was as follows: six cores were obtained from the peripheral zone (PZ) consisting of the para-midline, the middle and the lateral part, in addition to two cores from the transition zone (TZ) in each lobe. In patients with abnormalities on baseline or postcontrast ultrasonography, 2 to 4 additional cores were sampled targeting the abnormalities. During the biopsy, the probe was rotated and angulated to the desired sagittal plane and the needle was introduced on the same plane. After the biopsy gun was fired, the probe was switched to a convex transducer to detect the biopsy needle and the most closely corresponding transverse images with the same gland morphologic findings in postcontrast images were reproduced and saved for further correlation with regions of interest (ROIs). To facilitate the spatial correlation of the contrast and biopsy images, similar depth and focus settings were used to obtain similar transverse images (Fig.

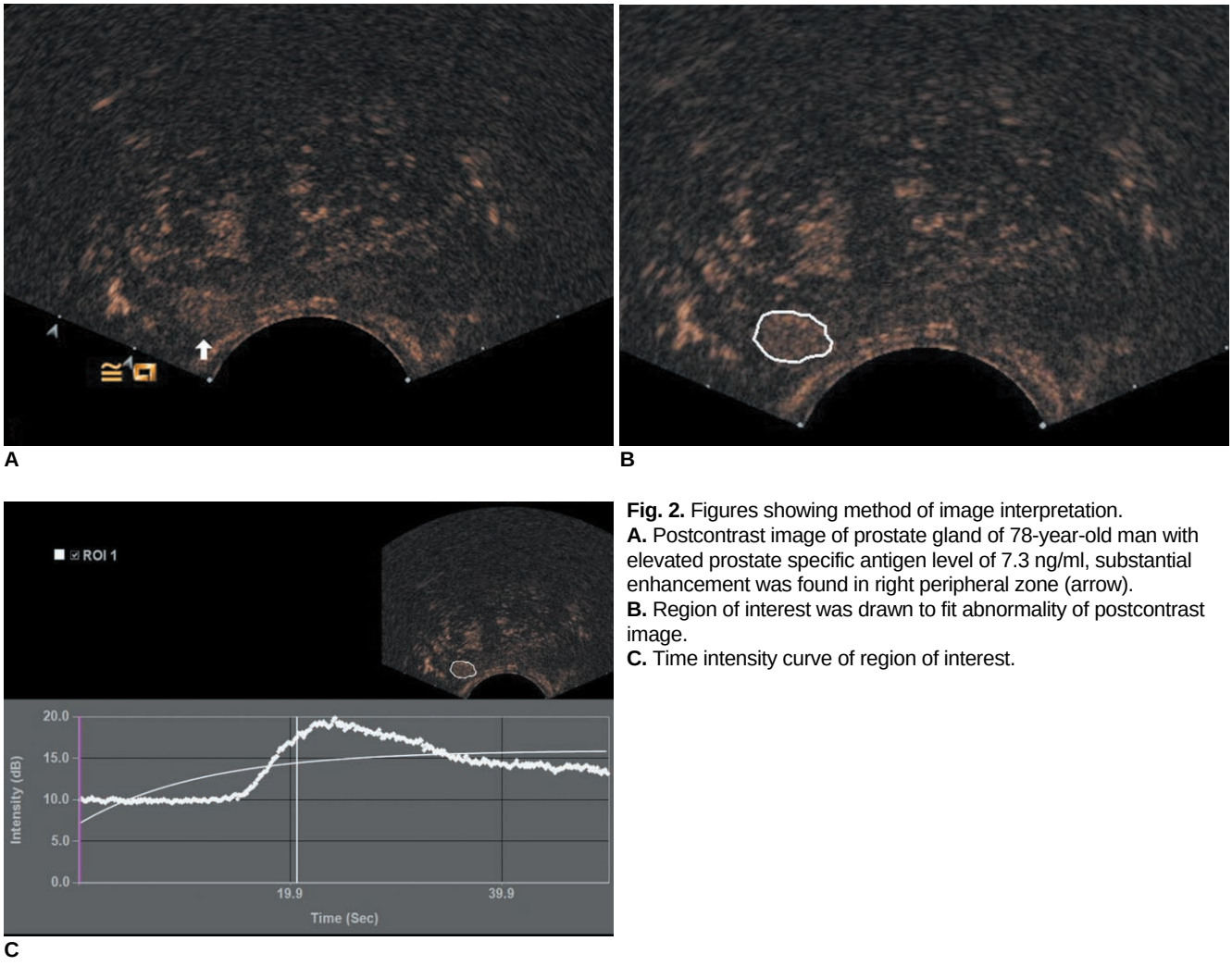

A B C

Fig. 2. Figures showing method of image interpretation.
A. Postcontrast image of prostate gland of 78-year-old man with elevated prostate specific antigen level of 7.3 ng/ml, substantial enhancement was found in right peripheral zone (arrow).
B. Region of interest was drawn to fit abnormality of postcontrast image.
C. Time intensity curve of region of interest.

1).

All specimens were marked as to the site of origin and analyzed separately. The pathological findings were categorized as malignant with an assigned Gleason score for each biopsy core, prostatic intraepithelial neoplasia, benign prostate hyperplasia, and inflammation. Prostate cancers with a Gleason score of 7 or above were categorized as high grade tumors while the rest were categorized as low grade tumors.

Image Interpretation

All contrast-enhanced ultrasound data were analyzed on the workstation using the Axius ACQ software (TOMTEC, Germany) by one radiologist who was blinded to all clinical and pathological information. The suspicion of carcinoma included the presence of an echotexture abnormality or contour deformity on grayscale images consisting of an increased or asymmetric flow pattern on Doppler images and substantial or heterogeneous enhancement on postcontrast images. For abnormal ultrasound findings above, ROIs were drawn to fit the sonographic abnormalities (Fig. 2). The ROIs were also drawn for each octant systematic biopsy site and the diameters were set to approximately 4 mm. The spatial correlation of the biopsy site and the ROI placement was based on the reproduced transverse images of the biopsy needle (Fig. 3). The time intensity curve was reconstructed for each ROI and the curve characteristics were described using the hemodynamic indices: arrival time (AT), is the time when the signal in the ROI has grown by 20% (in seconds), time-to-peak (TTP), indicates the moment of maximum enhancement (in seconds), peak intensity (PI), shows the value of the maximum intensity in the ROI that occurs after time zero (in dB).

Statistical Analysis

Differences between two groups (high grade and low grade cancer) were analyzed using student's *t*-test or Mann-Whitney test. A Chi-square test was used to compare the rate between groups. Spearman correlation

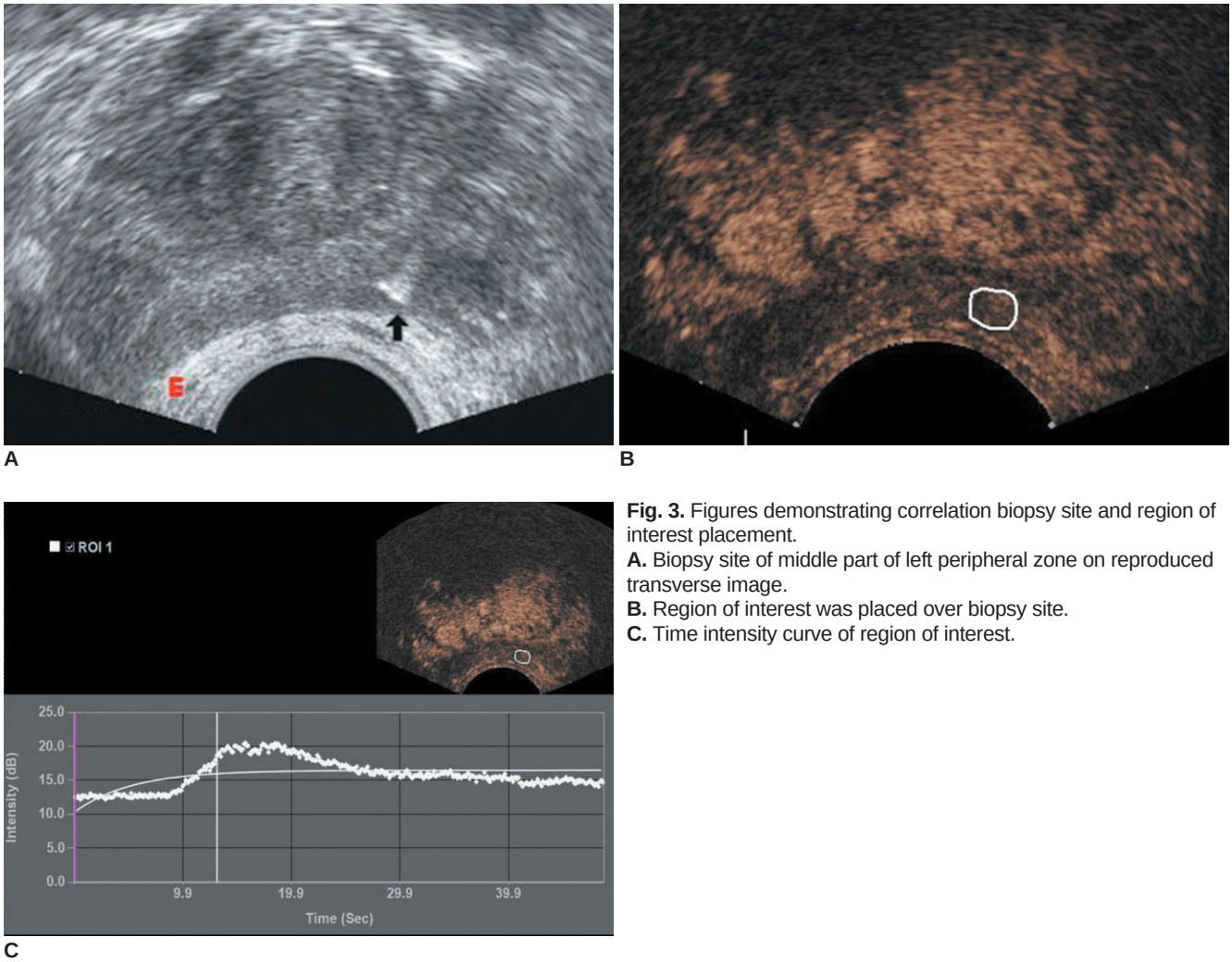

A B C

Fig. 3. Figures demonstrating correlation biopsy site and region of interest placement.
A. Biopsy site of middle part of left peripheral zone on reproduced transverse image.
B. Region of interest was placed over biopsy site.
C. Time intensity curve of region of interest.

coefficients were calculated to assess whether there is a correlation between the hemodynamic indices and biopsy Gleason score. *P*-values less than 0.05 were considered statistically significant, and all statistical analyses were performed using SPSS version 13.0 (SPSS, Chicago, IL).

RESULTS

Among the 103 patients tested, the prostate biopsies revealed 41 patients with prostate cancer and 62 patients with non-malignant prostate disease. Of the 62 patients with non-malignant prostate disease, 58 enrolled subjects had a PSA velocity < 10% after a one-year follow-up. Two of the patients had noticeably elevated serum PSA levels during a follow-up examination (41.12, 11.64 ng/ml before the biopsy and 97, 25.13 ng/ml after one-year follow-up). In addition, two patients were lost in the follow-up and were excluded. Thus, we excluded these four patients. In 58 non-malignant patients that underwent prostate biopsies, 38 revealed a benign prostate hyperplasia, whereas 20 were identified as having a benign prostate hyperplasia with inflammation cell infiltration.

In total, the prostate biopsies revealed 154 prostate cancer lesions in 41 prostate cancer patients, including 29 Gleason score 9 lesions, 29 Gleason score 8 lesions, 65 Gleason score 7 lesions, and 31 Gleason score 6 lesions. In addition, 125 prostate cancer lesions were in the PZ and 29 were in the TZ. Also, in the 154 prostate cancer lesions, 47 were biopsy-proven malignant sonographic abnormalities and 107 were positive systematic cores. The clinical characteristics of the patients were described in Table 1.

Significant differences in the hemodynamic indices were observed between the biopsy sites of non-malignant prostate disease patients and prostate cancer lesions (Table 2). The characteristics of the hemodynamic indices of the biopsy sites of non-malignant patients, low-grade prostate cancer lesions, and high-grade lesions were described in Table 3. High-grade tumors showed earlier enhancement and earlier arrival of peak enhancement than low-grade tumors. No significant difference for the PI was observed between two groups ($p = 0.158$). Moreover, no significant differences were found in hemodynamic indices between the biopsy sites of non-malignant patients and low-grade prostate cancer lesions.

Table 1. Clinical Characteristics of Patients

Variable	Non-Malignant Patients	Prostate Cancer Patients	*P* value
No. of patients	58	41	
Age years mean ± SD (range)	67.76 ± 8.91 (45–83)	73.61 ± 6.39 (59–86)	0.001#
PSA ng/ml mean ± SD (range)	8.44 ± 4.10 (0.30–16.80)	26.00 ± 28.54 (4.27–100)	< 0.001#
PSAD ng/ml per ml mean±SD (range)	0.20 ± 0.13 (0.01–0.56)	0.69 ± 0.82 (0.1–3.8)	< 0.001#
DRE (%)	10 (17%)	22 (54%)	0.001*

Note.— **P* value by Chi-square, #*P* values by Mann-Whitney test, PSA = prostate specific antigen, PSAD = PSA density, DRE = digital rectal examination

Table 2. Comparison of Hemodynamic Indices between Biopsy Sites of Non-Malignant Patients and Prostate Cancer Lesions

Variable	Non-Malignant	Prostate cancer	*P* value
AT (sec) mean ± SD	23.36 ± 6.76	21.15 ± 4.78	< 0.001
TTP (sec) mean ± SD	31.62 ± 8.47	28.56 ± 6.36	< 0.001
PI, dB mean ± SD	7.69 ± 4.19	9.70 ± 4.01	< 0.001

Note.— *P* value by student's *t*-test, AT = arrival time, TTP = time-to-peak, PI = peak intensity, sec = second

Table 3. Comparison of Hemodynamic Indices between Biopsy Sites of Non-Malignant Patients, Low-Grade Prostate Cancer Lesions and High-Grade Prostate Cancer Lesions

Variable	Non-Malignant (Group 1)	Low-Grade Prostate Cancer (Group 2)	High-Grade Prostate Cancer (Group 3)	*P* value (Group 1 versus 2)	*P* value (Group 2 versus 3)	*P* value (Group 1 versus 3)
AT (sec) mean±SD	23.36 ± 6.76	23.59 ± 5.88	20.53 ± 4.26	0.982	0.001	< 0.001
TTP (sec) mean±SD	31.62 ± 8.47	31.65 ± 7.72	27.78 ± 5.75	0.854	0.002	< 0.001
PI, dB mean±SD	7.69 ± 4.19	8.79 ± 4.55	9.92 ± 3.85	0.161	0.158	< 0.001

Note.— *P* value by student's *t*-test, AT = arrival time, TTP = time-to-peak, PI = peak intensity

Prostate cancer lesions located in the PZ were analyzed separately (Table 4). In addition to shorter AT and TTP, high-grade PZ tumors had a higher PI than low-grade tumors ($p = 0.009$), while low-grade tumors in the PZ also had higher PI than the PZ of non-malignant patients ($p = 0.022$). The scatter plot diagrams of the PZ hemodynamic indices were shown in Figure 4. The correlations between the PZ prostate cancer Gleason score and hemodynamic indices were analyzed and the results indicated an increase in PZ cancer Gleason score with increasing PI and a decrease in AT and TTP (Spearman correlation coefficient 0.223, −0.335 and −0.351, respectively) ($p = 0.013$, < 0.001 and < 0.001 respectively).

Table 4. Comparison of Hemodynamic Indices between PZ Biopsy Sites of Non-Malignant Patients, Low-Grade PZ Prostate Cancer Lesions and High-Grade PZ Prostate Cancer Lesions

Variable	Non-Malignant PZ (Group 1)	Low-Grade PZ Prostate Cancer (Group 2)	High-Grade PZ Prostate Cancer (Group 3)	*P* value (Group 1 versus 2)	*P* value (Group 2 versus 3)	*P* value (Group 1 versus 3)
AT, s mean±SD	24.48 ± 6.95	24.13 ± 6.25	20.75 ± 4.40	0.808	0.002	< 0.001
TTP, s mean±SD	32.27 ± 8.68	31.36 ± 7.83	27.59 ± 5.74	0.617	0.008	< 0.001
PI, dB mean±SD	5.78 ± 2.49	7.02 ± 3.45	9.16 ± 3.57	0.022	0.009	< 0.001

Note.— *P* value by student's *t*-test, AT = arrival time, TTP = time-to-peak, PI = peak intensity, PZ = peripheral zone

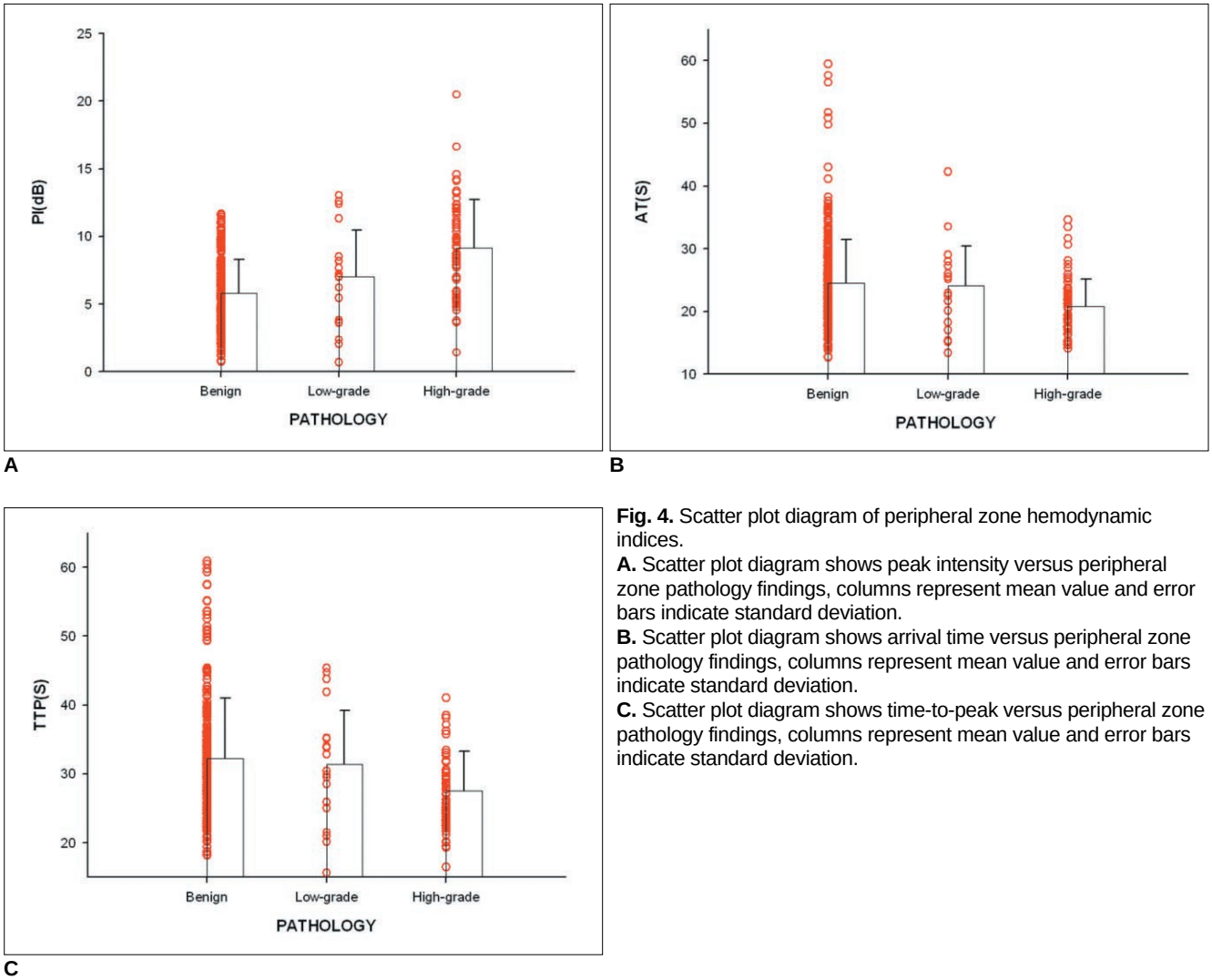

Fig. 4. Scatter plot diagram of peripheral zone hemodynamic indices.
A. Scatter plot diagram shows peak intensity versus peripheral zone pathology findings, columns represent mean value and error bars indicate standard deviation.
B. Scatter plot diagram shows arrival time versus peripheral zone pathology findings, columns represent mean value and error bars indicate standard deviation.
C. Scatter plot diagram shows time-to-peak versus peripheral zone pathology findings, columns represent mean value and error bars indicate standard deviation.

DISCUSSION

One of the most challenging characteristics of prostate cancer is its variable biologic aggressiveness. Prostate cancer tends to have increased vascularity compared to healthy prostatic tissue due to the formation of new vessels or an increase in the capacity of existing vessels. Wilson and his colleagues revealed that prostate cancer lesions with a higher Gleason score had a higher degree of vascularity (1). Further studies also concluded that microvessel density was related to pathological stage, disease recurrence, and disease specific survival (11–13). Contrast-enhanced ultrasonography, which is useful in assessing microvessel density, shows its potential value in predicting prostate cancer Gleason score.

Recent studies suggested that contrast-enhanced ultrasonography was more sensitive for the detection of clinically significant prostate cancer. Mitterberger and his colleagues (10) performed contrast-enhanced color Doppler targeted biopsies plus 10-core systematic biopsies in 690 patients suspected of having prostate cancer. Contrast-enhanced color Doppler targeted biopsies detected significantly higher Gleason scores compared with systematic biopsies. The author concluded that contrast-enhanced color Doppler biopsies seemed to be helpful in the grading of prostate cancer. The development in computer software provided the ability to reconstruct time-intensity curves and hemodynamic indices. In a retrospective study, Goossen et al. (14) found that the minimal time to the peak was the most predictive parameter for localization of the prostate cancer lesions, but the correlation between prostate cancer Gleason score and hemodynamic indices was not included in their study.

Compared with Doppler imaging employed by most previous studies (7–9, 14), the CPS harmonic imaging used in this study recognizes and processes the unique nonlinear fundamental and higher order harmonic signals generated by the contrast agent, thus allowing for a significant

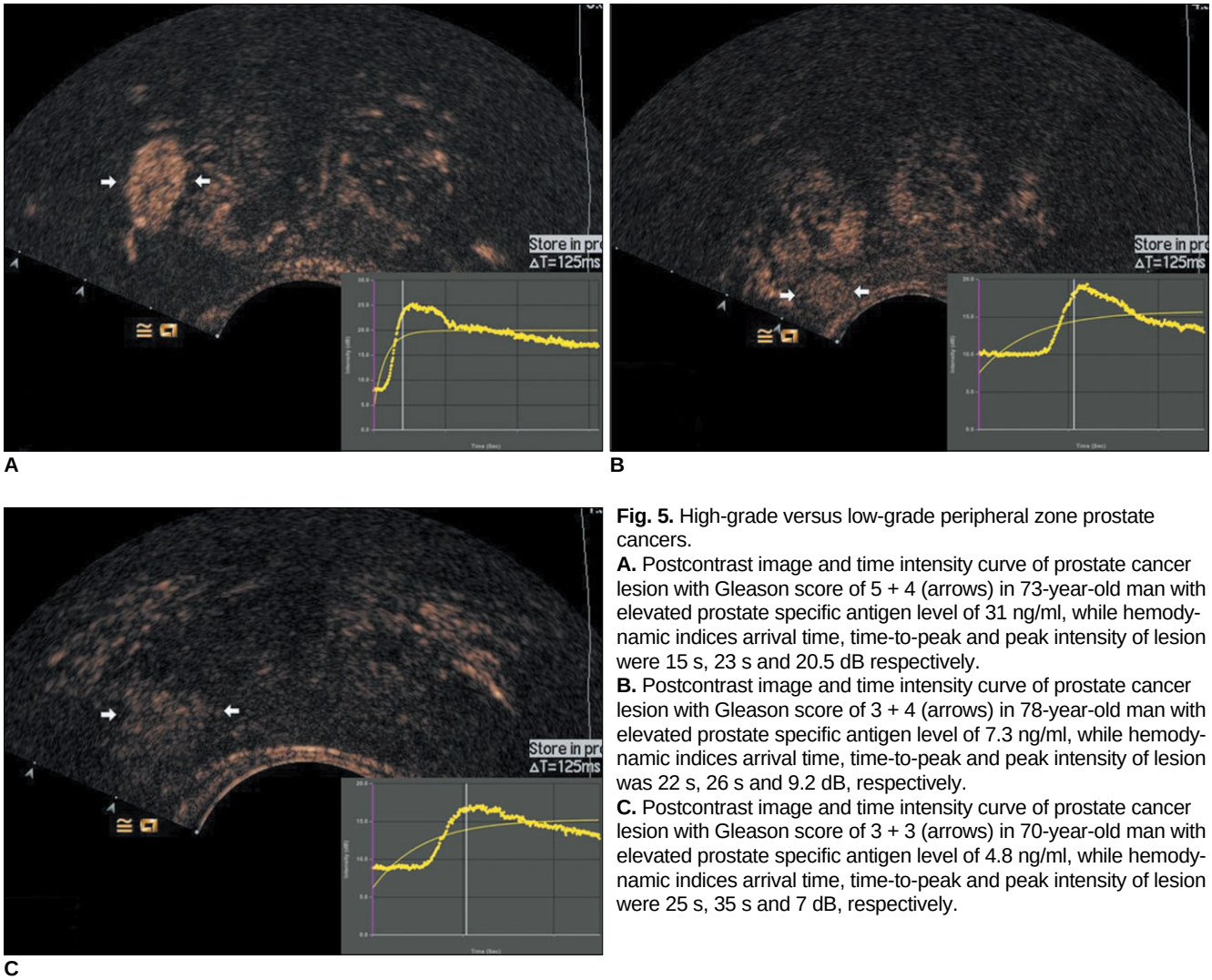

Fig. 5. High-grade versus low-grade peripheral zone prostate cancers.
A. Postcontrast image and time intensity curve of prostate cancer lesion with Gleason score of 5 + 4 (arrows) in 73-year-old man with elevated prostate specific antigen level of 31 ng/ml, while hemodynamic indices arrival time, time-to-peak and peak intensity of lesion were 15 s, 23 s and 20.5 dB respectively.
B. Postcontrast image and time intensity curve of prostate cancer lesion with Gleason score of 3 + 4 (arrows) in 78-year-old man with elevated prostate specific antigen level of 7.3 ng/ml, while hemodynamic indices arrival time, time-to-peak and peak intensity of lesion was 22 s, 26 s and 9.2 dB, respectively.
C. Postcontrast image and time intensity curve of prostate cancer lesion with Gleason score of 3 + 3 (arrows) in 70-year-old man with elevated prostate specific antigen level of 4.8 ng/ml, while hemodynamic indices arrival time, time-to-peak and peak intensity of lesion were 25 s, 35 s and 7 dB, respectively.

increase in the specificity of contrast agent-to-tissue, even at low mechanical index power levels. Furthermore, gray-scale CPS imaging is less affected by motion noise and blooming artifact. Therefore, CPS harmonic imaging is more sensitive in depicting neovascularity associated with prostate cancer.

This study focuses evaluating the utility of contrast-enhanced ultrasonography for predicting prostate cancer aggressiveness. The results revealed that in high-grade tumors, the contrast-enhanced blood arrived, and was distributed to the tissue more quickly than in low-grade tumors. This might be related to the development of immature vascularity associated with the growth of malignancies. No significant difference was observed for the PI between the low and high-grade tumor groups. When TZ prostate cancer lesions were excluded, we found that high-grade PZ tumors had a higher PI than low-grade PZ tumors, in addition to shorter AT and TTP (Fig. 5). This might be explained by the fact that the TZ of the prostate gland often showed hypervascularity because of the changes of the benign prostatic hyperplasia. Moreover, PZ prostate cancer lesions with higher Gleason scores had a higher degree of vascularity, while the parameter PI was thought to be associated with the blood volume in the area. We also demonstrated that there was a trend toward increasing the PZ prostate cancer Gleason score with increasing PI and decreasing AT and TTP, while the Spearman correlation coefficient was 0.223, −0.335, and −0.351, respectively. The correlation coefficients indicated that there were overlaps between the hemodynamic indices at various Gleason score levels; however, this might reflect methodologic and physiologic variations.

In this study, a different instrument was used to perform transperineal prostate biopsies, which is the routine biopsy protocol at our institute. For the transperineal protocol, the cores from any given area of the prostate can be attained with this procedure because the needle is freely handed, thus allowing for better targeting of the abnormal findings in the lateral part of the gland (15). Furthermore, transperineal cores were taken along a longitudinal plan parallel to the rectum, while the whole core was obtained from the PZ (16). In contrast, transrectal cores are taken along a plane crossing the PZ and often involving the TZ in the distal end of the core, especially in larger prostates where the PZ is only a thin layer compressed by the TZ (15). This may result in the overestimation of the PZ prostate cancer lesions and misplacement of the ROI. The transfer of the abnormalities of the endfire probe onto the image of the biplane probe used for prostate biopsies was currently a manual process that would be susceptible to localization errors. To minimize these errors, 2 to 4 additional cores were sampled to target the abnormalities. Moreover, the location of each biopsy site was confirmed at transverse images after the biopsy gun was fired.

Our study did have some limitations which may have caused the overlaps between the hemodynamic indices at various Gleason score levels. First, the contrast-enhanced ultrasonography was performed with an endfire probe, while the prostate biopsy was performed with a biplane probe. The probe transfer increased the likelihood of introducing localization errors. Second, the ROIs averaging with surrounding tissue might have contributed to scatter in the hemodynamic indices, especially in smaller lesions. Third, although the pressure of the transrectal probe was controlled to a minimum by the elimination of gas between the rectal wall and the probe to obtain more perfusion of the paramidline segment, relative hypovascularity in the prostate cancer lesions of paramidline segment was observed in some cases. This can be partially attributed to the near-field effect, which is difficult to avoid. Finally, the arrival and distribution of contrast-enhanced blood to the prostate gland is affected by the circulation system of each patient, which cannot be controlled and represents a source of variation in the results.

Moreover, in our study, the biopsy Gleason score was used to correlate with the CPS indices. Although a prostate biopsy Gleason score is widely used in assessing prostate cancer aggressiveness, a biopsy specimen still represents a limitation for the assessment of all cancer sites and grades. Gleason score is sometimes under or upgraded after radical prostatectomy (17, 18). However, the result of this present study was based on the correlation between the ROI and biopsy site, not all the cancer lesions, thus was less affected by under or upgrading.

In conclusion, CPS harmonic ultrasonography can be used to image the hemodynamic behavior of prostate cancer and the CPS imaging indices correlate with the pathologic Gleason scores. Although there are overlaps between hemodynamic indices at various Gleason score levels, the results still suggests a measurable potential for the use of CPS harmonic ultrasonography for the assessment of noninvasive prostate cancer aggressiveness.

References

1. Wilson NM, Masoud AM, Barsoum HB, Refaat MM, Moustafa MI, Kamal TA. Correlation of power Doppler with microvessel density in assessing prostate needle biopsy. *Clin Radiol* 2004;59:946-950
2. Volavsek M, Masera A, Ovcak Z. Incidental prostatic carcinoma. A predictive role of neoangiogenesis and comparison with other prognostic factors. *Pathol Oncol Res* 2000;6:191-196
3. Goldberg BB, Liu JB, Forsberg F. Ultrasound contrast agents: a review. *Ultrasound Med Biol* 1994;20:319-333
4. Halpern EJ. Contrast-enhanced ultrasound imaging of prostate

cancer. *Rev Urol* 2006;8:S29-S37
5. Ko EY, Lee SH, Kim HH, Kim SM, Shin MJ, Kim N, et al. Evaluation of tumor angiogenesis with a second-generation US contrast medium in a rat breast tumor model. *Korean J Radiol* 2008;9:243-249
6. Lee SH, Suh JS, Shin MJ, Kim SM, Kim N, Suh SH. Quantitative assessment of synovial vascularity using contrast-enhanced power Doppler ultrasonography: correlation with histologic findings and MR imaging findings in arthritic rabbit knee model. *Korean J Radiol* 2008;9:45-53
7. Frauscher F, Klauser A, Volgger H, Halpern EJ, Pallwein L, Steiner H, et al. Comparison of contrast enhanced color Doppler targeted biopsy with conventional systematic biopsy: impact on prostate cancer detection. *J Urol* 2002;167:1648-1652
8. Pelzer A, Bektic J, Berger AP, Pallwein L, Halpern EJ, Horninger W, et al. Prostate cancer detection in men with prostate specific antigen 4 to 10 ng/ml using a combined approach of contrast enhanced color Doppler targeted and systematic biopsy. *J Urol* 2005;173:1926-1929
9. Roy C, Buy X, Lang H, Saussine C, Jacqmin D. Contrast-enhanced color Doppler endorectal sonography of prostate: efficiency for detecting peripheral zone tumors and role for biopsy procedure. *J Urol* 2003;170:69-72
10. Mitterberger M, Pinggera GM, Horninger W, Bartsch G, Strasser H, Schäfer G, et al. Comparison of contrast enhanced color Doppler targeted biopsy to conventional systematic biopsy: impact on Gleason score. *J Urol* 2007;178:464-468
11. Bono AV, Celato N, Cova V, Salvadore M, Chinetti S, Novario R. Microvessel density in prostate carcinoma. *Prostate Cancer Prostatic Dis* 2002;5:123-127
12. Bostwick DG, Wheeler TM, Blute M, Barrett DM, MacLennan GT, Sebo TJ, et al. Optimized microvessel density analysis improves prediction of cancer stage from prostate needle biopsies. *Urology* 1996;48:47-57
13. Borre M, Offersen BV, Nerstrøm B, Overgaard J. Microvessel density predicts survival in prostate cancer patients subjected to watchful waiting. *Br J Cancer* 1998;78:940-944
14. Goossen TE, de la Rosette JJ, Hulsbergen-van de Kaa CA, van Leenders GJ, Wijkstra H. The value of dynamic contrast enhanced power Doppler ultrasound imaging in the localization of prostate cancer. *Eur Urol* 2003;43:124-131
15. Emiliozzi P, Corsetti A, Tassi B, Federico G, Martini M, Pansadoro V. Best approach for prostate cancer detection: a prospective study on transperineal versus transrectal six-core prostate biopsy. *Urology* 2003;61:961-966
16. Emiliozzi P, Longhi S, Scarpone P, Pansadoro A, DePaula F, Pansadoro V. The value of a single biopsy with 12 transperineal cores for detecting prostate cancer in patients with elevated prostate specific antigen. *J Urol* 2001;166:845-850
17. Pinthus JH, Witkos M, Fleshner NE, Sweet J, Evans A, Jewett MA, et al. Prostate cancers scored as Gleason 6 on prostate biopsy are frequently Gleason 7 tumors at radical prostatectomy: implication on outcome. *J Urol* 2006;176:979-984
18. Steinberg DM, Sauvageot J, Piantadosi S, Epstein JI. Correlation of prostate needle biopsy and radical prostatectomy Gleason grade in academic and community settings. *Am J Surg Pathol* 1997;21:566-576